


Thermal and dynamic mechanical behavior of poly(lactic acid) (PLA)-based electrospun scaffolds for tissue engineering

Nicola Ciarfaglia^{1,2} | Antonio Laezza² | Louise Lods¹ | Antoine Lonjon¹  | Jany Dandurand¹ | Antonietta Pepe² | Brigida Bochicchio²

¹CIRIMAT, Physique des polymères, Université Paul Sabatier, Toulouse, France

²Laboratory of Bioinspired Materials, Università degli Studi della Basilicata, Potenza, Italy

Correspondence

Antoine Lonjon, CIRIMAT, Physique des polymères, Université Paul Sabatier, 31062 Toulouse Cedex 09, France.
Email: antoine.lonjon@univ-tlse3.fr

Abstract

Electrospun scaffolds can find numerous applications, including biomedical; for example, tissue engineering. Poly-L-lactic acid is considered suitable for these applications, but its low-thermal stability and its poor mechanical properties limit this polymer use. The aim of this work is to obtain a modulation of the final scaffolds characteristics such as fibers dimension, wettability, elasticity, and resistance to rupture through the choice of the polymers to be electrospun. Different electrospun scaffolds containing gelatin, Poly-DL-lactic acid, different percentages of cellulose nanocrystals and an elastin peptide have been produced. Thermal stability, physical structure, and its mechanical behavior have been studied. Results suggest that the electrospun scaffolds show better thermal and mechanical properties than bulk materials; that is, the scaffolds with the best hydrophilic and thermomechanical properties are the samples containing 3% (wt/wt) of CNCs and elastin peptide.

KEYWORDS

biomaterials, degradation, differential scanning calorimetry, fibers, mechanical properties

1 | INTRODUCTION

Electrospinning is widely used to produce materials made of fibers with regular diameters ranging from 2 nm to several micrometers from solutions of polymers under a strong electric field in the order of thousands of Volts. The added value of electrospinning consists in the possibility to easily tune fibers diameter and porosity, that is, the ratio between the volume of voids called pores and the total volume of the material considered, together with the surface-to-volume ratio as well.¹ These findings are considered appealing characteristics in the perspective of the use of electrospun fibers as potential tools in biomedical devices and innovative materials as well. For example, they are known as biomedical devices,² used in drug

delivery and tissue engineering,³ and as filters, protective textile, catalysts and storage cells for hydrogen fuel cells.⁴ Furthermore, in the last decades electrospun fibers were widely investigated because their production requires minimum consumption of solvents.⁵

In the last few years, many electrospun scaffolds have been successfully produced from different polymers, such as polyamide 11 for kidney cells culturing,⁶ poly-(vinylidene fluoride), in order to enhance the piezoelectric-phase,⁷ polyurethane for bone tissue regeneration,⁸ poly(–caprolactone) for potential dental applications,⁹ and in blends with polyethylene glycol as a drug delivery system,¹⁰ and many others.

Furthermore, it is even possible to electrospun blends of polymers, as done for example by Oliveira Lobo et al.¹¹

and by Zhang et al.,¹² which produced matrices of biological interest.

Poly-L-lactic acid (PLA) is the best candidate of polymers used for the production of electrospun scaffolds. Actually, it is considered ideal for biomedical applications and tissue engineering.^{13–15} Nevertheless, it is weak for the low-thermal stability and the poor mechanical properties, which make difficult its use in biomedical applications. The choice of proper polymeric blend could affect the mechanical properties of the scaffold. For example, silicon dioxide nanoparticles,¹⁶ or cellulose nanocrystals (CNCs) have been used as nanofillers for their ability to confer strength to the material.¹⁷

CNCs are the product of hydrolysis of cellulose fibers composed of amorphous and crystalline regions.¹⁸

Several papers concern the use of CNCs and nanowhiskers as reinforcing agents of polymeric matrices composed of polyvinyl acetate, polyethylene oxide.^{19–22} Finally, CNCs was added to PLA in electrospun scaffolds, for applications in tissue engineering.²³

The aim of this work is to elaborate scaffold nature-inspired and biodegradable polymers. The working hypothesis was the modulation the properties such as fibers dimension, wettability, elasticity, and mechanical properties.

Other components that can improve mechanical properties of electrospun fibrous structures are natural proteins, including collagen, gelatin (GE), and elastin.²⁴ Taking advantage of these studies, herein different bio-inspired electrospun scaffolds were produced and characterized through thermomechanical techniques. Six kinds of different polymeric matrices were electrospun starting from polymeric blends of different hydrophobicity degree. All of them were solubilized in 1,1,1,3,3,3 Hexafluoro-2-Propanol (HFP). The polymers were chosen as a function of biodegradable and biocompatible properties. First of all, GE was appealing for the presence of bioactive motifs and for its low immunogenicity.²⁵ Poly-lactic acid was herein used in the racemic form (PDLLA). As a matter of fact, PDLLA [Poly(D,L-lactic)acid] with a lower crystalline level undergoes faster degradation than semi-crystalline PLA.²⁶ That characteristic let it be preferred in the field of the tissue engineering.²⁷ Elastin is a highly hydrophobic and cross-linked protein assembled from a soluble precursor protein called tropoelastin. It is the protein responsible for the elasticity of vertebrates' tissue such as large blood vessels, lung, and skin. It was ascertained that the conformational features related to the single exon coded polypeptides are the same as those suggested when they are insert in the entire protein, because each exon encodes an independent and self-contained structure. Therefore, it is possible to use the exon-by-exon analysis to study the characteristics of a single domain. In the works

of Tamburro et al., a coherent recomposition of the elastin domains, with the intention of giving an acceptable solution of the elastin structure–function problem was proposed.^{28,29} Finally, a peptide encoded by exon 15 (EX15) of Human Tropoelastin and CNCs at 1, 3, 5, and 8% (compared to the weight of the other components) were added to the polymeric blends in order to improve biocompatibility and strength, respectively. Due to GE solubility in water and in biological fluids, a cross-linking reaction was carried out on the electrospun scaffolds.

The scaffolds produced in this work are reported, in order to facilitate reading, with names that give information about their composition. Letters G, P, and N mean “Gelatin GE”, “Polymer PDLLA,” and “Nanocellulose CNCs” respectively, while the numbers represent CNCs percentage in the polymeric blends. Finally, prefix EI and suffix k meanings “elastin peptide” and “cross-linked,” respectively.

The morphology analysis of the samples was carried out by scanning electron microscopy (SEM) and from SEM images average fibers diameters were calculated. Thermal properties and hydrophilic degree of the electrospun scaffolds were assessed by thermogravimetric analysis (TGA) while the physico-chemical structure evolutions of the electrospun scaffolds (also after conducting the swelling test on them) were studied by differential scanning calorimetry (DSC) technique. Finally, Dynamic mechanical analysis (DMA) was used in order to investigate mechanical properties of the samples.

2 | EXPERIMENTAL

2.1 | Materials

GE (type B powder, 225 Bloom strength, p.I. 3.8–5.5 at 25°C) from bovine skin, was bought from Sigma Aldrich (St. Louis, MO); Poly-DL-Lactic Acid (PDLLA EasyFil PLA–PolyLactic Acid, transparent pellets, molecular weight 126,000 g/mol, density 1240 Kg/m³) was purchased from Form Futura (Netherlands), cellulose nanocrystals (CNCs, spray dried powder, particle size 1–50 µm, pH in water 6–7, 88% crystalline fraction) was obtained from CelluForce (Montreal, Quebec, Canada) while elastin peptide was synthesized as previously reported.²⁹ For electrospinning, all the components were dissolved in 1,1,1,3,3,3 Hexafluoro-2-Propanol (HFP) (Iris Biotech GMBH, Marktredwitz, Germany). For cross-linking, *N*-hydroxysuccinimide (NHS) was obtained from Sigma Aldrich, *N*-(3-dimethylaminopropyl)-*N'*-ethylcarbodiimide hydrochloride (EDC·HCl) was purchased from Novabiochem (Darmstadt, Germany) and ethanol was bought from Carlo Erba Reagents (Cornaredo, MI).

2.2 | Fabrication of PLA-based scaffolds

2.2.1 | Electrospinning

GP mixture (GE:PDLLA ratio 1:3, 12.0% wt/vol) was prepared by dissolving GE in HFP at 37°C for 2 h and then adding PDLLA. The mixture was kept at 37°C under magnetic stirring for 3 h. All the NGP mixtures (1NGP, 3NGP, 5NGP, and 8NGP) were obtained by dispersing CNCs in HFP at room temperature and by keeping the dispersions under magnetic stirring for 24 h. The blends underwent some sonication cycles. Later, GE was dissolved in the polymeric mixtures and kept under stirring for 2 h at 37°C. Finally, PDLLA was added and stirred for 3 h at 37°C.

In E18NGP mixture (EX15:CNCs:GE:PDLLA ratio 1:7.5:22.5:67.5, 13.1% wt/vol) elastin peptide and GE were added at the same time.

The polymeric mixtures were loaded into a 5 ml plastic syringe with a 18 G stainless steel and then electrospun at 19 kV (gamma high-voltage generator), with a flow of the volumetric pump of 1.6 ml/h. The target was a copper plate covered with an aluminum sheet with a distance from the needle of 19 cm. Example of GP, 8NGP, and E18NGP scaffolds composition is listed in Table 1.

2.2.2 | Cross-linking

Electrospun scaffolds were cross-linked using a 45.0 mM EDC/NHS (1:1) 85.5% ethanolic solution. Scaffolds were left at room temperature under stirring on an orbital shaker (PSU-10i, Biosan, Riga, Latvia) for 24 h at 60 rpm, then washed with deionized H₂O (20 ml × 3 times) to remove the residual crosslinker and finally dried in 95.0% ethanol (1 h at 60 rpm).

3 | METHODS

3.1 | Scanning electron microscopy

The morphological analysis was carried out using a Jeol (Japan) JSM7800F Prime scanning electron microscope and SEM images were acquired with a voltage of 3 kV,

after platinum metallization. The images were analyzed using ImageJ software (Java open source) supplied with DiameterJ plug-in.

3.2 | Thermogravimetric analysis

Thermal stability of the electrospun scaffolds was investigated by TGA using a Q50 device (TA Instruments, New Castle). Samples with a mass between 5 and 7 mg were cut from the board of the scaffolds and placed into the instrument under a synthetic air flow of 10 ml/min (oxidizing atmosphere). They were heated from room temperature to 700°C at 10°C/min. Three samples were analyzed for each electrospun scaffold.

3.3 | Differential scanning calorimetry

The physical structure was analyzed using DSC7 (Perkin Elmer) at a range of 30–200°C at 20°C/min under nitrogen flow. Samples with a mass ranging 4–7 mg were cut from the board of the scaffolds, and placed in closed aluminum pans. After the first scan, the samples were immediately cooled at the same rate, and the second scan was recorded. Glass transition temperature T_g and heat capacity jump ΔC_p were determined by the tangent method while the melting temperature T_m was taken at the maximum of the peak.

DSC measurement was conducted also after the swelling test on the electrospun scaffolds at low temperature with Diamond DSC (Perkin Elmer), under helium atmosphere. In this case, samples were placed in pans and hydrated with 30 μ l of ultrapure water. After the experiments we wait 60 min at 25°C in order to reproduce the swelling test. Two cooling scans were carried out, between 25 and –120°C, and 80 and –120°C at a rate of 10°C/min and two heating scans from –120 to 80°C and from –120 to 85°C at a rate of 10°C/min, with an identical empty reference pan.

3.4 | Dynamic mechanical analysis

DMA was conducted using an ARES G2 strain-controlled rheometer (TA Instruments). Samples dimensions were

TABLE 1 Polymeric blends compositions of GP, 8NGP, and E18NGP samples

Sample name	Gelatin (GE) mass (g)	Poly-DL-lactic acid (PDLLA) mass (g)	Cellulose nanocrystals (CNCs) mass (g)	Elastin peptide (EX15) mass (g)	Solvent (HFP) volume (ml)
GP	0.09	0.27	/	/	3.0
8NGP	0.09	0.27	0.03	/	3.0
E18NGP	0.09	0.27	0.03	0.0039	3.0

of $35 \times 12.5 \text{ mm}^2$ with a thickness of 0.3 mm for the non-cross-linked scaffolds and of 0.7 mm for those cross-linked. The scaffolds were analyzed in tensile geometry mode and the temperature range of the heating scans was performed between 0 and 80°C at a heating rate of $3^\circ\text{C}/\text{min}$. The strain and the frequency were fixed at 0.03% and 1 Hz respectively within the material linearity range. $E'_{\omega}(T)$ (elongational storage modulus) and $E''_{\omega}(T)$ (elongation loss modulus) were determined.

4 | RESULTS AND DISCUSSION

4.1 | Morphology observation

Scanning electron microscopy images were used in order to analyze electrospun fibers morphology before and after cross-linking reaction. In Figure 1(a), SEM image of GP scaffold is shown: it presented a well-defined three-

dimensional fibrillar microstructures and interconnected porous microstructures. A linear and random-oriented structure of the fibers was noted and the absence of solvent and beads suggested a good solubilization of the polymers in the blend. After the cross-linking reaction with EDC, the scaffold showed a change in the morphology (Figure 1(b)), with a more curvilinear trend of the fibers. These characteristics were also obtained in the work of Piccirillo et al., which prepared several electrospun scaffolds with different GE/PLA ratios.³⁰ GE can lead to the production of bead-free fibers and smooth morphology of the scaffolds even when it is electrospun in blend with polycaprolactone.³¹

Also for 8NGP scaffold (Figure 1(c)) as for GP one, a nonwoven matrix with fibrillar and interconnected porous microstructures presenting randomly oriented fibers was observed. CNCs were finely dispersed in the polymeric mixture because the presence of beads was not noted. In Figure 1(d) SEM image of 8NGPk scaffold is

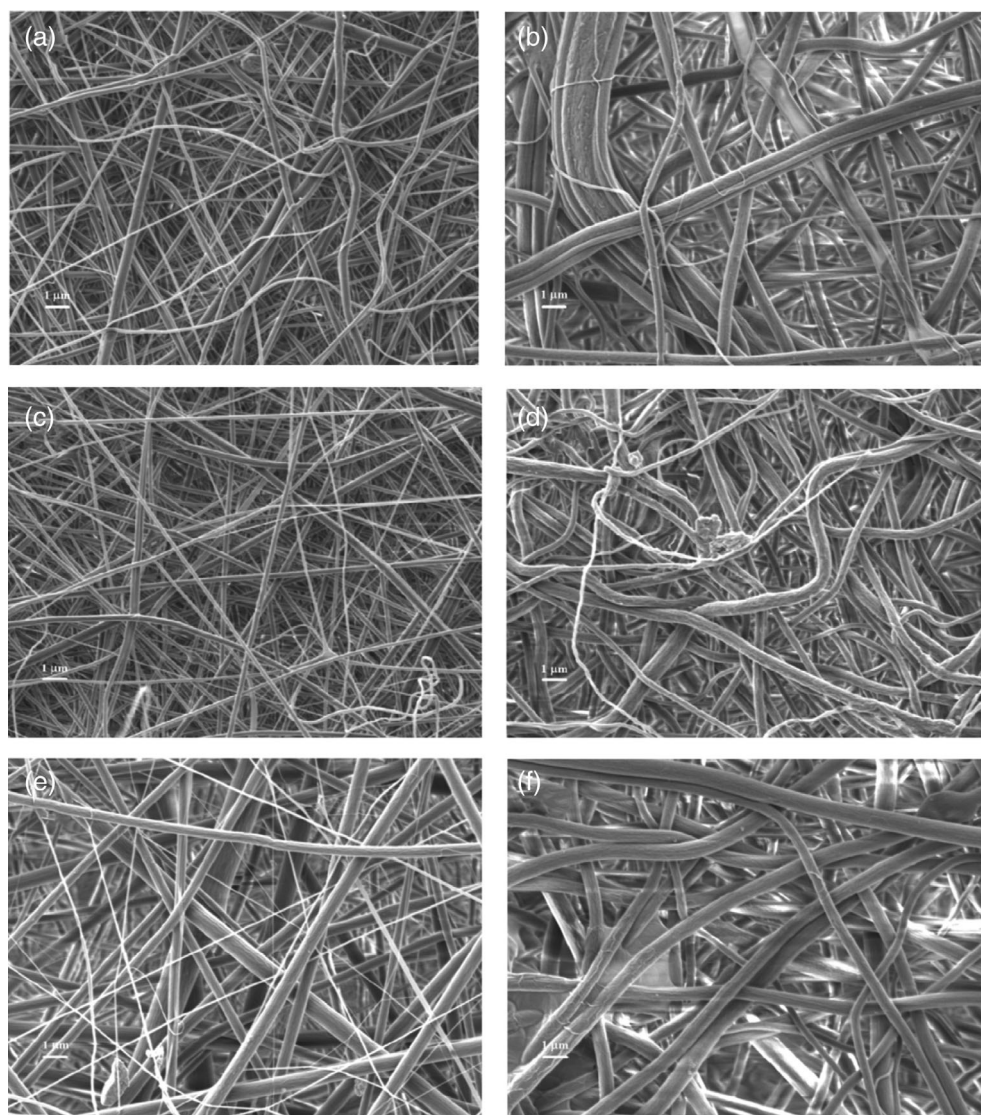


FIGURE 1 Scanning electron microscopy images of (a–b) GP, (c–d) 8NGP, and (e–f) El8NGP scaffolds before and after cross-linking reaction

presented: herein, there is again a different morphology, similar to that of the GPk sample, after cross-linking reaction, with a curvilinear trend of the fibers.

The other samples containing CNCs, that is, 1NGP, 3NGP, and 5NGP scaffolds, with their cross-linked fees, presented morphology very similar to 8NGP matrix (data not shown). This similarity in SEM images suggested that CNCs was well dispersed in the polymeric blends for all these concentrations, as confirmed by Yang et al.,³² who produced matrices composed of PLA and cellulose nanofibrils (CNFs) as nanofiller with concentrations of 3%, 5%, 7%, and 10% via electrospinning. CNFs have also been used in order to reinforce scaffolds made up of PLA and poly(butylene succinate) (PBS),³³ and other fibrous particules like carbon nanotubes (CNTs) and GE to blends of PLA have led to well-formed and uniform non-woven scaffold, thanks to their incorporation in the polymeric suspension.³⁴

These fibrillar beadless and interconnected porous microstructures were also found in EI8NGP samples (Figure 1(e)), with curled fibers after cross-linking (Figure 1(f)). Rnjak-Kovacina et al.,³⁵ and Jiménez Vázquez et al.³⁶ have developed electrospun scaffolds with fibers structure similar to ours samples and composed of human tropoelastin and collagen and bovine elastin and collagen derived from chicken skin, respectively.

From SEM analysis it can be concluded that all the samples showed a similar morphology and an analogous behavior after cross-linking reaction. The mean diameter value measured on 1000 fibers from three different images is around 1116 ± 290 nm.

4.2 | Thermal stability

In order to analyze the thermal stability of the samples, TGA was carried out under oxidizing atmosphere (synthetic airflow). For each electrospun scaffolds, three analysis were done.

In Figure 2 a comparison between TGA thermograms of respectively GP, 8NGP, and EI8NGP scaffolds is presented.

This graph shows the normalized weight and the derivative thermogravimetric (DTG) curves in function of the temperature. On GP scaffold (Figure 2), three main thermal phenomena were noted. The first one was observed at a maximum of intensity at about 63°C due to the loss of the water present in the matrix. In fact, despite PDLA is essentially a hydrophobic polymer, the presence of the hydrophilic regions of GE (which is partially hydrolyzed collagen) increased the ability of the electrospun scaffold to bind water. In literature this

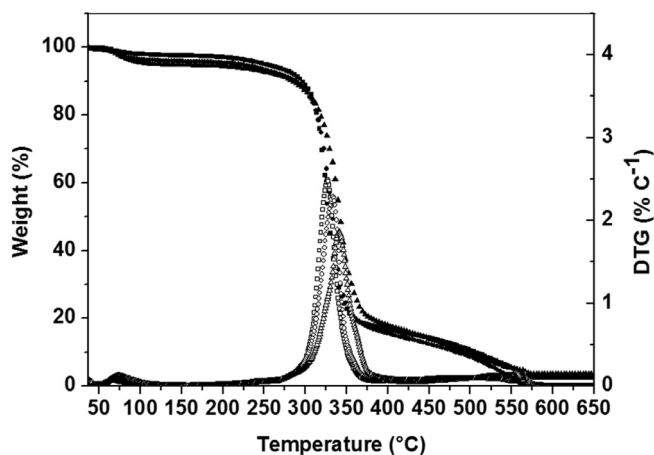


FIGURE 2 Comparison of thermal behavior by TGA thermograms of the three typologies of the electrospun scaffolds. Loss mass and derivated loss mass are reported ($10^\circ\text{C}/\text{min}$). Square, circle, and up triangle, represents GP, 8NGP, and EI8NGP samples respectively. Loss mass is reported as filled symbols, while derivated loss mass is reported as empty symbols. TGA, thermogravimetric analysis

TABLE 2 Degradation temperature, calculated using derivated loss mass curves and percentage of water lost, calculated on the TGA thermograms

Scaffold	Degradation temperature ($^\circ\text{C}$)	Lost water (%)
GP	327.1 ± 0.3	-2.2
GPk	327.4 ± 0.7	~ 0
1NGP	332.6 ± 0.5	-4.3
1NGPk	333 ± 2	-1.8
3NGP	338 ± 2	-5.1
3NGPk	330 ± 6	-1.7
5NGP	329 ± 4	-4.4
5NGPk	326.1 ± 0.3	-2.2
8NGP	331 ± 4	-3.7
8NGPk	330 ± 5	~ 0
EI8NGP	335.8 ± 0.8	-4.6
EI8NGPk	334.1 ± 0.8	~ 0

desorption phenomenon was observed when GE was electrospun.³⁷ The main degradation started at a temperature around 250°C and reached a maximum of intensity at $327.1 \pm 0.3^\circ\text{C}$, (Table 2) with the loss of about 80% of the scaffold mass.

Subsequently, a high-temperature degradation phenomenon (deriving from the oxidation of the first degradation residue) with a lower slope of the normalized weight curve, was present and led to the total

decomposition of the sample, at a temperature around 560°C. The same trend for 8NGP and El8NGP scaffolds can be noted, with an increase of the degradation temperature with the presence of elastin peptide ($335.8 \pm 0.8^\circ\text{C}$).

CNCs have been used as nanofiller even in the case of electrospun scaffolds made up of GE.³⁸

We have tested various contains of CNCs in our scaffolds. The scaffolds named 1NGP, 3NGP, and 5NGP, which contain a percentage of CNCs of 1%, 3%, and 5% (wt/wt) respectively, presented thermograms very similar (data not shown). Table 2 shows the values of thermal degradation. For the first two typologies of mats, an increase of degradation temperature, which reached the maximum value of $338 \pm 2^\circ\text{C}$ for the 3NGP scaffold was observed. This increased temperature with the presence of CNCs is in agreement with the works of Shi et al.,³⁹ and Zhou et al.,⁴⁰ in electrospun blends of PLA with different amounts of CNCs. When the amount of added CNCs became higher (scaffolds 5NGP and 8NGP) a decrease of the degradation temperature was observed.

Therefore, the presence of the CNCs, up to 3% (wt/wt) seems to improve the thermal stability of the matrices, probably due to char formation from CNCs before the thermal decomposition of GP scaffold, inhibiting the thermal conductivity and then leading to a decrease of the degradation temperature of these scaffolds.⁴¹ In literature a decrease of mechanical properties is described after the percolation threshold.⁴²

Also the peptide effect seems to improve the thermal stability of the samples. As a matter of fact, if we compare 8NGP and El8NGP, we note an increase of 5°C for degradation temperature. The slight increase could be explaining by a better crosslinking induced by the presence of peptide. A higher crosslinking provides more cohesion between polymer chains. This cohesion increase needs more energy to obtain the thermal degradation.

Figure 3 shows the TGA thermograms before and after cross-linking reaction for 8NGP scaffold.

The main difference between these two samples was the water content in the matrix. The scaffold cross-linked did not show loss of water in this case.

Table 2 highlights how the quantity of water present in the electrospun scaffolds increases with the addition of CNCs and elastin peptide: 3NGP and El8NGP scaffolds showed the maximum percentage of water, 5.1% and 4.6% respectively. This behavior was probably due to the presence of the hydroxyl groups of CNCs and to the hydrophilic regions of the peptide, which can better form hydrogen bonds with water, leading to a higher hydrophilicity of the scaffolds. The finding that all the cross-linked samples showed a smaller presence of water can be explained by the fact that cross-linking induces a decrease of hydrophilic sites and of mobility.

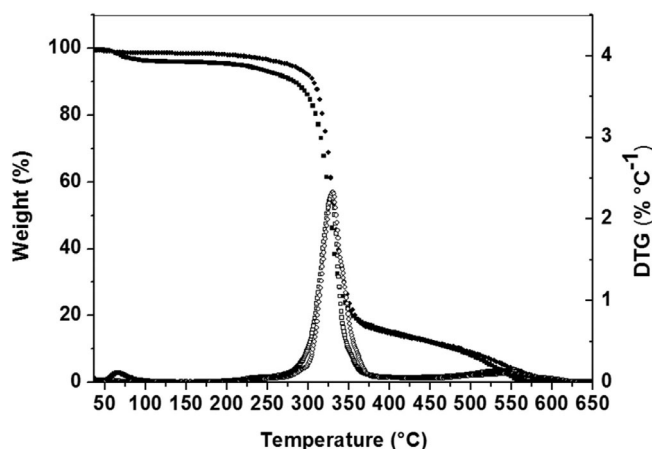


FIGURE 3 Comparison between the TGA thermograms of 8NGP electrospun scaffolds before (square) and after (circle) cross-linking reaction. Loss mass is reported as filled symbols, while derivated loss mass is reported as empty symbols. TGA, thermogravimetric analysis

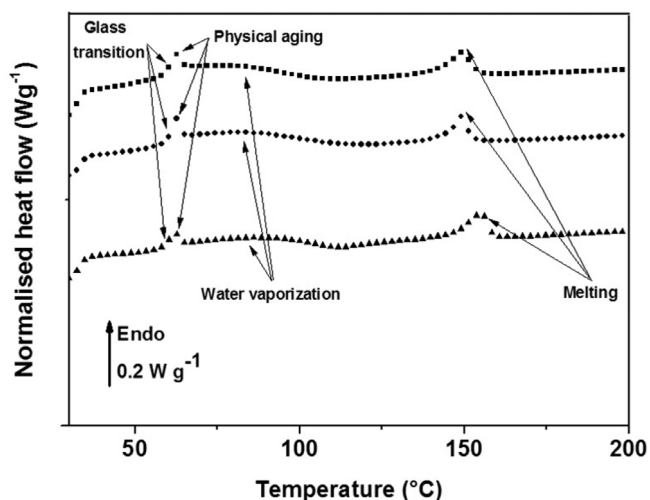


FIGURE 4 First heating thermograms of non-cross-linked electrospun scaffolds performed at $20^\circ\text{C}/\text{min}$. Square, circle, and up triangle represents GP, 8NGP, and El8NGP samples respectively

4.3 | Physical structure

Figure 4 presents the first heating scans of non-cross-linked electrospun scaffolds (GP, 8NGP, and El8NGP). The thermal parameters of all samples are reported in Table 3.

The scaffolds showed a glass transition temperature, near 56°C associated with amorphous phase and a peak is superimposed on the heat capacity step attributed to the physical aging. We can note only one T_g , consistent with a good miscibility of the two polymers. In GE/PLA blends Alipilakkotte noted that the miscibility was

TABLE 3 DSC measurements (1st and 2nd refer to first and second heating scan, respectively)

Scaffold	T_g ($^{\circ}\text{C}$)		T_m ($^{\circ}\text{C}$)		ΔC_p ($\text{J g}^{-1} \text{C}^{-1}$)		χ_c (%)
	1st	2nd	1st	2nd	1st	2nd	
GP	56.6	51.7	148.9	/	0.6	0.3	19.6
GPk	61.9	50.7	149.0	/	0.8	0.2	15.9
1NGP	52.9	52.4	155.1	144.7	0.6	0.2	29.1
1NGPk	58.0	53.7	156.3	146.7	0.5	0.3	18.9
3NGP	54.0	53.8	155.3	149.1	0.6	0.2	24.2
3NGPk	54.4	44.6	154.7	/	0.7	0.2	19.0
5NGP	52.3	51.5	155.0	144.1	0.6	0.3	29.5
5NGPk	60.4	50.7	156.9	144.3	0.7	0.3	17.5
8NGP	58.7	53.2	149.0	/	0.8	0.3	13.8
8NGPk	63.3	52.4	156.2	145.7	0.7	0.2	20.0
EI8NGP	57.8	54.8	154.9	145.1	0.5	0.3	16.3
EI8NGPk	62.8	52.3	156.1	146.3	0.7	0.3	15.6

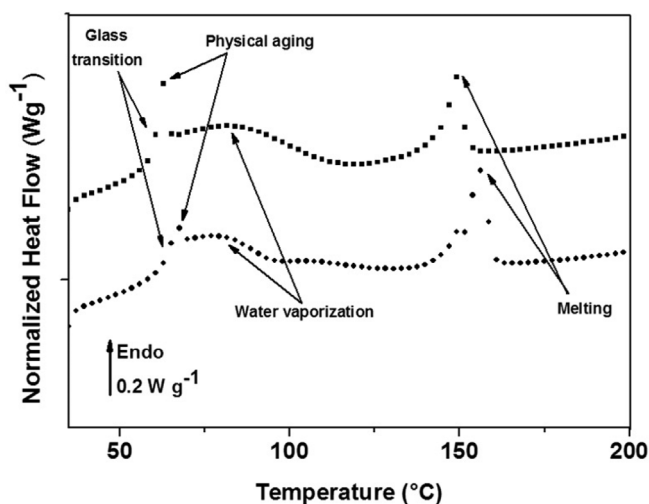


FIGURE 5 First heating DSC thermograms of 8NGP electrospun scaffolds before (square) and after (circle) cross-linking reaction. DSC, differential scanning calorimetry

achieved when the GE was covalently grafted on the PLA surface.⁴³ Physical aging phenomenon was observed in all samples on the first heating scans and the T_g value was measured between 52.3 and 63.3 $^{\circ}\text{C}$ (Table 3).

The presence of interstitial water was confirmed by the broad complex endothermic peak located in a temperature range between 70 and 150 $^{\circ}\text{C}$. At high temperature, a melting peak was observed at around 149 $^{\circ}\text{C}$ indicative of crystalline phase. Mukherjee et al. obtained T_m values ranging from 102 to 104 $^{\circ}\text{C}$ from the analysis of pigskin GE.⁴⁴

With the addition of CNCs, the melting temperature was measured between 149 and 155 $^{\circ}\text{C}$. A similar T_m was registered by Muijca-Garcia et al.,⁴⁵ in PLA-CNCs

nanocomposite fibers via melt-spinning. It interesting to note that add elastin peptide drive to an analogous T_m .

In the second heating scans the endothermic event at the glass transition vanishes and the data, listed in Table 3 shown a good stability of glass transition temperature with the low level of nanocellulose, and a decrease of 5 $^{\circ}\text{C}$ of T_g in scaffolds with 8% of CNCs or elastin peptide. The melting temperature decrease strongly when it can be measured.

In Figure 5 we compared the 8NGP scaffold first heating scan before and after cross-linking reaction.

We can observe an increase of both thermal transitions, glass, and melting. The values reported in Table 3 confirm this increase of thermal properties for all the samples. But it seems to be that the crystalline phase (T_m values) was less affected than amorphous phase (T_g values) by the cross-linking.

In the second heating scans, the glass transition temperature of all the cross-linked scaffolds, decrease until 3NGPk when at higher concentrations T_g increases again: this finding suggests that a percolation threshold phenomenon is present at 3% CNCs (wt/wt). This phenomenon was observed for example when CNTs were added in polymeric matrices.^{42,46} Finally, T_m value decreases at about 100 $^{\circ}\text{C}$ in the second heating scan.

This study shows that the different products used for the scaffold formulation have a good miscibility. In the first heating ramp, we observed the sample fingerprint linked to process and composition. Physical aging phenomenon observed superimposed at the glass transition is due to the electrospinning process, and can make difficult T_g measurement with good accuracy, this endothermic fingerprint vanishes which thermal cycling. An addition of CNCs to PDLLA and GE with various ratio

formed a hydrogen bonding network, restricting the segmental mobility retarding the cooperative motion of the polymer chains, and leading to the increase of glass transition temperature. A similar T_g behavior was observed by Cai et al.,⁴⁷ which produced electrospun scaffolds composed of poly-DL-lactic acid with a filler different from CNCs, that is, nanodiamonds. With elastin peptide the thermal response made unchanged.

A broad endothermic peak superimposed with several transitions (70 and 150°C) was attributed to the vaporization of bound water.

Cross-linking treatment induces an enhancement of thermal parameters, T_g (excepted 3%) and T_m . This result could be due to the effect of the cross-linking reaction of GE. In literature we found analogous results: with genipin cross-link GE electrospun scaffolds,⁴⁸ or the use of vinyltrimethoxysilane to form cross-linked bonds on PLA electrospun scaffolds.⁴⁹ In presence of elastin peptide not any specific behavior was observed.

A second heating scan modify significantly the thermal behavior of amorphous and crystalline phase of scaffolds, plasticization effect on amorphous phase and smaller crystals demonstrating the non-reversible effect of temperature on the electrospinning scaffold.

Adding elastin peptide at the formulation does not modify the thermal properties.

In Table 3 we reported also the calculated electrospun scaffolds crystallinity values, calculated from DSC, using the enthalpy of melting on first heating scan and the theoretical ΔH_m for a 100% crystalline PLA, 93 J/g.^{50,51} GP scaffold presented a crystallinity of 19.6%, for non-cross-linked samples, there was an increase of crystallinity with CNCs addition until 5NGP scaffold (29.5%), while, at 8% (wt/wt) concentration and with peptide addition crystallinity decreased, assuming values of 13.8% and 16.3%. This datum suggests that a low amount of CNCs could act as nucleating agent for improving the crystallization of PLA molecular chains,³⁹ and suggest that the increase of crystallinity could contribute to the enhance of degradation temperature,⁵² as found in TGA studies. On the

contrary, cross-linking reaction led to a decrease of crystallinity except for 8NGPk scaffold.

DSC was also used in order to analyze the thermal properties of the electrospun scaffolds after conducting the swelling test. The swelling test was done only on the cross-linked scaffolds (GE is water soluble without the cross-linking reaction). Results obtained are presented in Table 4.

The first heating run, bring to the fore the structural water melting T_m . For GPK scaffold it assumed a value of 10.3°C this value decreased with the addition of CNCs (samples 1NGPk, 3NGPk, and 5NGPk), but became higher in 8NGPk scaffold and peptide addition at 9.2°C. The same trend has been found for the second heating scan. Using ImageJ software (Java open source) supplied with the DiameterJ plug-in, average fibers diameter were calculated from SEM images of the electrospun scaffolds and the DSC swelling test values, and listed with their SD, in Table 4. It is interesting to note that it seems to be a correlation between the structural water melting temperature and the scaffolds average fibers diameter: as a matter of fact the bigger is the average fibers diameter, the smaller is T_m . This result suggests that during the cooling scan water molecules could rearrange themselves better, leading to a higher crystallinity and to a higher T_m of the water, if the fibers diameter was smaller.

4.4 | Dynamic mechanical behavior

Mechanical properties of the scaffolds were analyzed by DMA. In Figure 6 storage modulus E' and loss modulus E'' are reported as a function of the temperature for GP, 8NGP, 8NGPk, and EI8NGP electrospun scaffolds.

In Figure 6, the viscoelastic step associated with the anelastic manifestation of glass transition call α mode, is visible on storage modulus. The temperature of α relaxation is consistent with previous calorimetric results. For 8% CNCs addition the glassy plateau decreases strongly, and the α relaxation is increased. Add elastin peptide at this ratio (EI8NGP) enhanced the modulus in the whole temperature range, and shifted α relaxation to a lower

Scaffold	T_m H ₂ O (°C)		ΔH (J/g)		Average fibers diameter (μm)
	1st	2nd	1st	2nd	
GPK	10.3	11.3	244.9	241.8	0.9 ± 0.2
1NGPk	7.3	6.6	267.9	231.6	1.6 ± 0.9
3NGPk	8.3	8.0	182.9	173.8	1.7 ± 0.4
5NGPk	5.8	7.4	264.2	260.3	2.2 ± 0.3
8NGPk	10.8	10.3	209.5	205.4	0.8 ± 0.3
EI8NGPk	9.2	8.8	178.3	176.9	1.2 ± 0.3

TABLE 4 Transition temperatures and melting enthalpies of water present in the electrospun scaffolds after swelling test found by using DSC

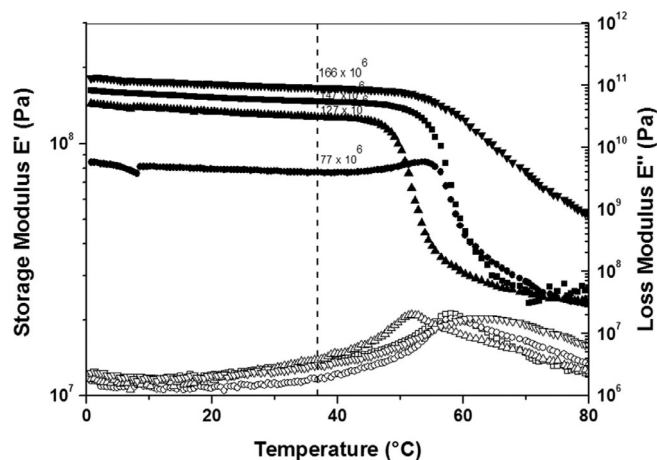


FIGURE 6 DMA thermograms of GP (square), 8NGP (circle), El8NGP (up triangle), and 8NGPk (down triangle) electrospun scaffolds. Storage moduli are reported in filled symbols while loss moduli are reported in empty symbols. DMA, dynamic mechanical analysis

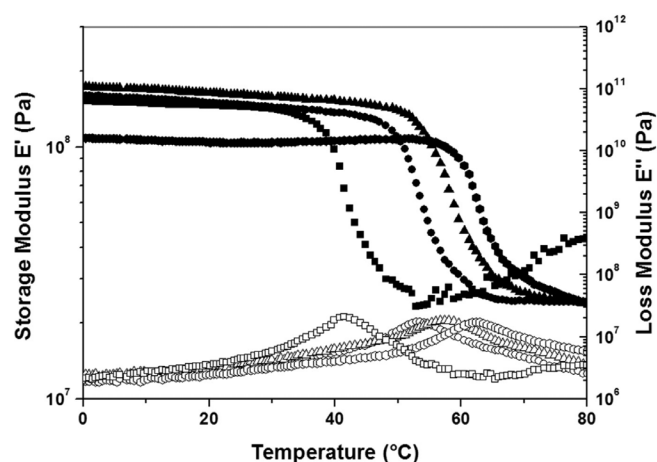


FIGURE 7 Effect of percentage of cellulose nanocrystals on the DMA behavior of scaffolds: DMA thermograms of GP (square), 1NGP (circle), 3NGP (triangle), and 5NGP (exagon) electrospun scaffolds. Storage moduli are reported in filled symbols while loss moduli are reported in empty symbols. DMA, dynamic mechanical analysis

temperature. Cross-linking treatment enhances the glassy and the rubbery plateau and α relaxation at this ratio.

The influence of CNCs added at GP is studied and reported in Figure 7.

We observed that α relaxation increases with increasing the nanocellulose ratio, and the glassy modulus increases until 3% of CNCs and decreases strongly for higher ratio. This datum is in agreement with the work of Pirani et al.,⁵³ which presented biodegradable nanocomposites of CNCs and electrospun PLA and found the maximum value of the storage modulus at a CNCs loading level of 3% (by the weight). An increase of E' has

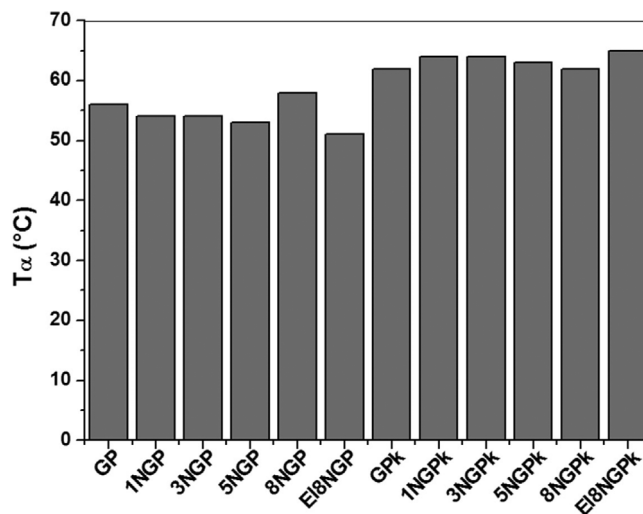


FIGURE 8 Histogram of T_α values obtained for the scaffolds studied in this work

also been observed when CNCs was used as reinforcing agent in electrospun poly(ϵ -caprolactone) nanofibers.⁵⁴

T_α values extracted from loss modulus E'' maximum are reported in Figure 8.

We can observe a continuous increase of T_α with increasing CNCs ratio. A decrease of this parameter appears adding elastin peptide, and finally the cross-linking treatment enhances T_α to 10°C. This behavior was consistent with calorimetric parameters and associated with the macromolecules mobility loss, and with the increase of the stiffness due to the reticulation. Glassy modulus observed around 150 MPa at low level of CNCs shown an important decrease (around 100 MPa) after 3% this value corresponds at a percolation threshold, and can give rise to a modulation of the mechanical properties. Uniaxial tensile testing of the scaffold in the dry state, previously described (Ciarfaglia et al.), showed that addition of 8% of CNC, both in the presence and absence of elastin peptide reduced significantly Young's moduli, thus increasing elasticity, while in the hydrated state no differences were observed. Interestingly, 8NGPk and El8NGPk scaffolds showed higher elongation at break inferring a role as plasticizer in the dry state.⁵⁵

Our scaffolds are suitable to be useful in skin tissue engineering; natural skin possesses tensile modulus between 15 and 150 MPa,^{17,56,57} and tunable adding CNCs or peptide with or without cross-linking. Our values are measured in dry state. Lower values are expected in physiological environment due to the plasticization effect.

5 | CONCLUSIONS

In this work, thermomechanical properties of different electrospun scaffolds, composed of GE, Poly-DL-Lactic

Acid, various ratio of CNCs and an Elastin peptide were analyzed. All the components of the polymeric blends showed a good miscibility. CNCs and elastin peptide were well dispersed in the solvent: their addition to the mixtures changed the concentration blends but did not affect their properties and the electrospinning process. SEM images showed a well-defined three-dimensional fibrillar microstructures and interconnected porous microstructures, with a more curvilinear trend after cross-linking reaction. TGA presented an increase of degradation temperature and hydrophilic properties with addition of CNCs up to 3% (wt/wt) and elastin peptide. By using DSC it was found an increase of the T_g with CNCs addition for the scaffolds series. Furthermore, a correlation between water melting temperature and fibers diameter average, after the swelling test, has been found. Finally, DMA showed an important increase of the T_α after the cross-linking and brought to the fore a concentration threshold on storage modulus values.

These results suggest that the electrospun scaffolds show better thermal and mechanical properties than bulk materials and the scaffolds 3NGP and El8NGP have the more interesting parameters for application. Therefore, these polymeric blends are useful for the preparation of electrospun scaffolds biocompatible and suitable for applications in the field of tissue engineering. Further studies will be conducted to check the biocompatibility of these matrices.

ORCID

Antoine Lonjon  <https://orcid.org/0000-0002-4346-6543>

REFERENCES

- [1] N. Bhardwaj, S. C. Kundu, *Biotechnol. Adv.* **2010**, *28*, 325.
- [2] L. Shang, Y. Yu, Y. Liu, Z. Chen, T. Kong, Y. Zhao, *ACS Nano* **2019**, *13*, 2749.
- [3] W. Cui, Y. Zhou, Y. Chang, *Sci. Technol. Adv. Mat.* **2010**, *11*, 1.
- [4] T. Subbiah, G. S. Bhat, R. V. Tock, S. Parameswaran, S. S. Ramkumar, *J. Appl. Pol. Sci.* **2005**, *96*, 557.
- [5] S. Thenmozhi, N. Dharmaraj, K. Kadirvelu, H. Y. Kim, *Mater. Sci. Eng., B* **2017**, *217*, 36.
- [6] M. Dhanalakshmi, A. K. Lele, J. P. Jog, *Mater. Today Com.* **2015**, *3*, 141.
- [7] M. Sharma, V. Srinivas, G. Madras, S. Bose, *RSC Adv.* **2016**, *6*, 6251.
- [8] C. Y. Chao, M. P. Mani, S. K. S. Jaganathan, *PLoS One* **2018**, *13*, 1.
- [9] A. Baranowska-Korczyn, A. Warowicka, M. Jasiurkowska-Delaporte, B. Grze'skowiak, M. Jarek, B. M. Maciejewska, J. Jurga-Stopa, S. Jurga, *RCS Adv.* **2016**, *6*, 19647.
- [10] C. Repanas, V. F. Wolkers, O. Grishkov, M. Müller, B. Glasmaker, *J. Vet. Pharm.* **2015**, *1*, 1.
- [11] A. Oliveira Lobo, S. Afewerki, M. M. Machado de Paula, P. Gahnadian, F. R. Marciano, Y. S. Zhang, T. J. Webster, A. Kadhemosseini, *Int. J. Nanomed.* **2018**, *13*, 7891.
- [12] Y. Zhang, H. Ouyang, C. T. Lim, S. Ramakrishna, Z. M. Huang, *J. Biomed. Mater. Res. Part B: Appl. Biomater.* **2005**, *72* B, 156.
- [13] B. Gupta, N. Revagade, J. Hilborn, *Prog. Polym. Sci.* **2007**, *32*, 455.
- [14] K. Kim, M. Yu, X. Zong, J. Chiu, D. Fang, Y. S. Seo, I. S. Hsiao, B. Chu, M. Hadjiargyrou, *Biomaterials* **2003**, *24*, 4977.
- [15] F. Yang, R. Murugan, S. Wang, S. Ramakrishna, *Biomaterials* **2005**, *26*, 2603.
- [16] Q. Ma, B. Mao, P. Cebe, *Polymer* **2011**, *52*, 3190.
- [17] Y. Mo, R. Guo, J. Liu, Y. Lan, Y. Zhang, W. Xue, Y. Zhang, *Colloid Surface B* **2015**, *132*, 177.
- [18] L. Brinchi, F. Cotana, E. Fortunati, J. M. Kenny, *Carbohydr. Polym.* **2013**, *94*, 154.
- [19] G. Gong, J. Pio, A. P. Mathew, K. Oksman, *Compos. Part A* **2011**, *42*, 1275.
- [20] S. Geng, M. Haque, K. Oksman, *Compos. Sci. Technol.* **2016**, *126*, 35.
- [21] A. Gupta, W. Simmons, G. T. Schueneman, D. Hylton, E. A. Mintz, *ACS Sustainable Chem. Eng.* **2017**, *5*, 1711.
- [22] S. Changarn, J. D. Mendez, K. Shanmuganathan, E. J. Foster, K. Weder, P. Supaphol, *Macromol. Rapid Commun.* **2011**, *32*, 1367.
- [23] C. Zhang, M. R. Salik, T. M. Cordie, T. Ellingham, Y. Dan, L. S. Turng, *Mater. Sci. Eng. C* **2015**, *49*, 463.
- [24] S. Heydarkhan-Hagvall, K. Schenke-Layland, A. P. Dhanasopon, F. Rofail, H. Smith, B. M. Wu, R. Shemin, R. E. Beygui, W. R. MacLellan, *Biomaterials* **2008**, *19*, 2907.
- [25] X. Z. Shu, Y. Liu, F. Palumbo, G. D. Prestwich, *Biomaterials* **2003**, *24*, 3825.
- [26] S. Farah, D. G. Anderson, R. Langer, *Adv. Drug Delivery Rev.* **2016**, *107*, 367.
- [27] M. Savioli Lopes, A. L. Jardini, R. Maciel Filho, *Proc. Eng.* **2012**, *42*, 1402.
- [28] A. M. Tamburro, B. Bochicchio, A. Pepe, *Biochemistry* **2003**, *42*, 13347.
- [29] A. M. Tamburro, A. Pepe, B. Bochicchio, *Biochemistry* **2006**, *45*, 9518.
- [30] G. Piccirillo, M. V. Ditaranto, N. F. S. Feuerer, D. A. Carvajal Berrio, E. M. Brauchle, A. Pepe, B. Bochicchio, K. Schenke-Layland, S. Hinderer, *J. Mater. Chem. B* **2018**, *6*, 6399.
- [31] M. I. Hassan, L. H. Chong, S. Hinderer, N. Sultana, *ARPN J. Eng. Appl. Sci.* **2016**, *23*, 13604.
- [32] Z. Yang, X. Li, J. Si, Z. Cui, K. Peng, *J. Wuhan Univ. Technol.* **2019**, *34*, 207.
- [33] T. Abudula, U. Saeed, A. Memic, K. Gauthaman, M. A. Hussain, K. Al-Turaif, *J. Polym. Res.* **2019**, *26*, 1.
- [34] A. Magiera, J. Markowski, E. Menaszek, J. Pilch, S. Blazewicz, *J. Nanomater.* **2017**, *2017*, 1.
- [35] J. Rnjak-Kovacina, S. G. Wise, Z. Li, P. K. M. Maitz, C. J. Young, Y. Wang, A. S. Weiss, *Acta Biomater.* **2012**, *8*, 3714.
- [36] J. Jiménez Vázquez, E. S. M. Martínez, *J. Mater. Res.* **2019**, *34*, 2819.
- [37] D. M. Correia, J. Padrão, L. R. Rodrigues, F. Dourado, S. Lanceroz-Méndez, V. Sencadas, *Polym. Test.* **2013**, *32*, 995.
- [38] A. Hivechi, S. H. Bahrami, R. A. Siegel, *Int. J. Biol. Macromol.* **2019**, *124*, 411.
- [39] Q. Shi, C. Zhou, Y. Yue, W. Guo, Y. Wu, Q. Wu, *Carbohydr. Polym.* **2012**, *90*, 301.

- [40] C. Zhou, Q. Shi, W. Guo, L. Terrel, A. T. Qureshi, D. J. Hayes, Q. Wu, *ACS Appl. Mater. Interfaces* **2013**, *5*, 3847.
- [41] R. Liepins, E. M. Pearce, *Environ. Health Perspect.* **1976**, *17*, 55.
- [42] A. Lonjon, S. Barrau, E. Dantras, P. Demont, C. Lacabanne, *Eur. J. Electr. Eng.* **2009**, *12*, 423.
- [43] S. Alippilakkotte, L. Sreejith, *J. Appl. Polym. Sci.* **2018**, *135*, 1.
- [44] I. Mukherjee, M. Rosolen, *J. Thermal Anal. Calorim.* **2013**, *114*, 1161.
- [45] A. Muijca-Garcia, S. M. Hooshmand, J. M. Kenny, K. Oksman, L. Peponi, *RSC Adv.* **2016**, *6*, 9221.
- [46] D. Carponcin, E. Dantras, J. Dadurand, G. Aridon, F. Levallois, L. Cadiergues, C. Lacabanne, *J. Non-Cryst. Solids* **2014**, *19–25*, 392.
- [47] N. Cai, Q. Dai, Z. EWang, X. Luo, Y. Xue, F. Yu, *Fiber Polym.* **2014**, *15*, 2544.
- [48] S. Baiguera, C. Del Gaudio, E. Lucatelli, E. Kuevda, M. Boieri, B. Mazzanti, A. Bianco, P. Macchiarini, *Biomaterials* **2014**, *35*, 1205.
- [49] M. Rahmat, M. Karrabi, I. Ghasemi, M. Zandi, H. Azizi, *Mater. Sci. Eng. C* **2016**, *68*, 397.
- [50] E. W. Fisher, H. J. Sterzel, G. Wegner, *Kolloid- Z. Z. Polym.* **1973**, *251*, 980.
- [51] H. Simmons, P. Tiwary, J. E. Colwell, M. Kontopoulou, *Polym. Degrad. Stab.* **2019**, *166*, 248.
- [52] A. P. Kumar, D. Depan, N. S. Tomer, R. P. Singh, *Prog. Polym. Sci.* **2009**, *34*, 479.
- [53] S. Pirani, H. M. N. Abushammala, R. HaShaikeh, *J. Appl. Polym. Sci.* **2013**, *10*, 3345.
- [54] J. O. Zoppe, M. S. Peresin, Y. Habibi, R. A. Venditti, O. J. Rojas, *ACS Appl. Mater. Interfaces* **2009**, *9*, 1996.
- [55] N. Ciarfaglia, A. Pepe, G. Piccirillo, A. Laezza, R. Daum, K. Schenke-Layland, B. Bochicchio, *Appl. Polym. Mater.* **2020**, *2*, 4836.
- [56] G. H. Kim, S. Ahs, Y. Y. Kim, Y. Cho, W. Chun, *J. Mater. Chem.* **2011**, *21*, 6165.
- [57] W. Li, C. T. Laurencin, E. J. Catterson, R. S. Tuan, F. K. Ko, *J. Biomed. Mater. Res.* **2002**, *60*, 613.

How to cite this article: N. Ciarfaglia, A. Laezza, L. Lods, A. Lonjon, J. Dandurand, A. Pepe, B. Bochicchio, *J Appl Polym Sci* **2021**, e51313.
<https://doi.org/10.1002/app.51313>